Evaluating structural brain networks based on their performance in predicting functional connectivity

Fani Deligianni[1], Chris A. Clark[1], and Jonathan D. Clayden[1]
[1]*Institute of Child Health, UCL, London, United Kingdom*

Audience: To those interested in constructing structural brain networks and to their relation to functional connectivity.

Purpose: The reconstruction of structural brain networks from diffusion-weighted images (DWI) entails several methodological steps. These include a choice of tractography algorithm and graph description. Evaluating the effect of these approaches is not straightforward since there is not ground truth data. Phantoms neither capture the complexity of neuronal fibers in-vivo, nor they provide information about the functional importance of false positives or negatives in recovering structural networks. Furthermore, structural networks are described as graphs, which only summarize microstructural properties recovered via tractography. The edges of a brain graph may reflect the number of streamlines connecting each pair of regions or the average fractional anisotropy (FA) or mean diffusivity (MD) along the neuronal path. Some of these networks may be more or less capable of capturing changes across populations either due to disease, or developmental or aging processes. We hypothesize that a more accurate reconstructed structural network would be able to predict functional connectivity better. We evaluate how well structural brain networks predict functional connectivity based on sparse canonical correlation analysis (sCCA) [1, 2].

Methods: Imaging data was acquired from 13 healthy adults with a 1.5T clinical scanner. DWI: 60 non-collinear gradient directions, b=1000 s mm^{-2}, 2.5mm slice thickness, 240 mm FOV, voxel size of 2.5x2.5x2.5 mm and TR/TE=7300/81 msec, rs-fMRI: 125 volumes, TR/TE=3320/50 msec, slice thickness 3.0 mm, voxel size 3.0x3.0x3.0 mm, flip angle 90^0, FOV 192x192x108 mm, voxel matrix 64x64x36. T1-weighted whole-brain structural images were also obtained in all subjects. Each of the 13 subjects' acquisition includes three structural scans and two rs-fMRI scans.

We define cortical regions of interest (ROIs) in gray matter (GM) based on freesurfer parcellation of the T1-weighted images. Anatomical labels are propagated from T1 space to native space for both fMRI and DWI using non-rigid registration [3]. Preprocessing of fMRI data involves removing the first five volumes, motion correction, low pass filtering and spatial smoothing with FSL. To construct functional brain networks the fMRI signal is averaged across voxels within each GM ROI. The signal in white matter (WM) and cerebrospinal fluid is also averaged and along with the six motion parameters provided from FSL are linearly regressed out. Functional connectivity is estimated as the inverse covariance matrix, normalized to unit diagonal based on a shrinkage estimator [4]. Preprocessing of DWI involves eddy current correction and retrospective correction of the gradient vectors. Structural brain networks are derived with probabilistic tractography based on the ball-and-stick model [5, 6]. This results in thousands of streamlines that connect cortical regions via WM. Structural brain networks are described as graphs with nodes equal to the number of ROIs and edges defined with one of the following ways: **a)** NSTREAMS: The number of streamlines that connect each pair of regions divided by the average number of white matter voxels that surround these ROIs. **b)** WFA: Weighted average FA along the streamlines that connect each pair of regions. Each voxel within a neuronal path is weighted based the visitation map, which reflects the number of streamlines that pass through it. **c)** FA: Average FA along the streamlines that connect each pair of regions. **d)** WMD: Weighted average MD along the streamlines that connect each pair of regions. Weighting is based on a visitation map as for WFA. **e)** MD: Average MD along the streamlines that connect each pair of regions.

We use sCCA to learn sparse vectors u, v that maximize the linear relationship between structure, $\mathbf{X}$, and function, $\mathbf{Y}$, as in eq.1. This approach is based on lasso penalties c_1, c_2 that control sparsity [1]. Subsequently, functional connectivity $\hat{\mathbf{Y}}$ is predicted from an unseen structural connectivity matrix $\bar{\mathbf{X}}$ according to eq.2. $\mathbf{D}$ is a diagonal matrix with the canonical correlation scores. The distance between the predicted and the measured functional connectivity is estimated in eq.3 [7-9]. Variability along functional scans dominates the prediction performance [2]. To cancel out this variability we consider pairwise differences as in eq. 4. Therefore, M and M' stand for different approaches of estimating structural connectivity matrices, ie. NSTREAMS versus WFA.

$$\max_{u,v} u^T \mathbf{X}^T \mathbf{Y} v \;,\; \|u\|_1 \le c_1, \|v\|_1 \le c_2 \quad \textbf{[eq.1]} \qquad \hat{\mathbf{Y}} = \left(u\bar{\mathbf{X}}\right)^{-1} \mathbf{D} v^{-1} \quad \textbf{[eq.2]}$$

$$d\left(\hat{\mathbf{Y}},\mathbf{Y}\right) = \left\| \mathrm{tr}\left(\log\left(\mathbf{Y}^{-1/2}\hat{\mathbf{Y}}\mathbf{Y}^{-1/2}\right)\right)\right\| \quad \textbf{[eq.3]} \qquad D\left(M,M'\right) = d\left(\hat{\mathbf{Y}}\left\{\mathbf{X}^{M}\right\},\mathbf{Y}\right) - d\left(\hat{\mathbf{Y}}\left\{\mathbf{X}^{M'}\right\},\mathbf{Y}\right) \quad \textbf{[eq.4]}$$

Results: Firstly, we use leave-one-out cross-validation to predict functional connectivity for each structural connectivity matrix via eq. 2. We calculate the distance between measured and predicted functional connectivity matrix based on eq.3. Note that this is a distance metric and the smaller it is the more accurate the prediction. Subsequently, we estimate the differences in prediction performance *D{M,M'}: D{NSTREMS,WFA}, D{NSTREAMS,FA}, D{NSTREAMS,WMD}, D{NSTREAMS,MD}*. In fig. 1, we use violin plots to summarize these differences across scans and subjects. The results show that NSTREAMS produces more accurate functional brain networks. The more negative the difference the worse the performance of the structural network compared to NSTREAMS. WFA networks follow in performance and the rest: WMD, FA and MD perform similarly.

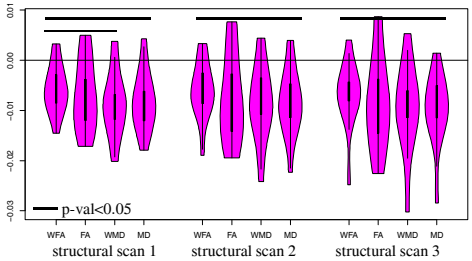

Fig.1: Differences in prediction performance between NSTREAMS and the other approaches as in eq. 4.

Fig. 2(â) shows the average rs-fMRI brain network. Brain regions are represented with spheres. Their centers and radius represent the center of masses of each underlying region and its relative size, respectively. The color-coding corresponds to different brain lobes. Fig. 2(a-e) shows the average structural brain networks constructed based on NSTREAM, WFA, FA, WMD and MD, respectively. It is apparent that in rs-fMRI the most prominent connections are inter-hemispheric, whereas in the structural networks are mostly intra-hemispheric. In fig. 2, the second line shows bootstrap results of 1000 iterations with replacement with repetition. We aim to identify the most prominent structural (u) brain connections, which are highly related to functional connectivity. In order to alleviate the influence of the lasso parameters c_1, c_2, we re-optimize them in each bootstrap iteration [1]. Finally, we estimate the probability of a connection to be present as the number of times it is selected divided by the number of total iterations. Fig. 2, bottom line, shows the structural connections with probability over 75%. The selected connections of NSTREAMS appear more stable.

Conclusions: We hypothesize that a more accurate and meaningful description of anatomical brain networks would perform better in predicting functional connectivity. We show statistically significant results that structural brain networks with edge weights that reflect number of streamlines perform best and they are followed by graphs based on weighted FA.

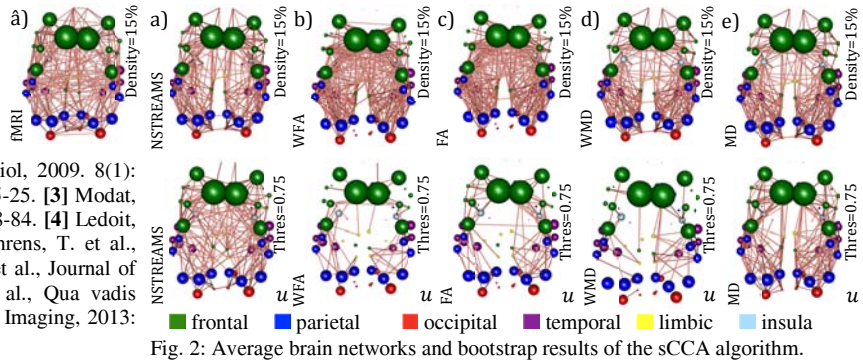

Fig. 2: Average brain networks and bootstrap results of the sCCA algorithm.

References: **[1]** Witten, D.M. et al., Stat Appl Genet Mol Biol, 2009. 8(1): Article 28. **[2]** Deligianni, F. et al., MICCAI-MBIA, 2013: 215-25. **[3]** Modat, M. et al., Comput Methods Programs Biomed, 2010. 98(3): 278-84. **[4]** Ledoit, O. et al., J Multivariate Anal, 2004. 88(2): 365-411. **[5]** Behrens, T. et al., Magnet Reson Med, 2003. 50(5): 1077-88. **[6]** Clayden, J.D. et al., Journal of Statistical Software, 2011. 44(8): 1-18. **[7]** Forstner, W. et al., Qua vadis geodesia, 1999: 113. **[8]** Deligianni, F. et al., IEEE Trans Med Imaging, 2013: in press. **[9]** Deligianni, F. et al., IPMI, 2011. 6801: 296-307.